PHYSICAL REVIEW B **77**, 064421 (2008)

Influence of MgO overlayers on the electronic states of Fe(001) thin films grown on GaAs(001)

Liu-Niu Tong,[1,2,3,*] Frank Matthes,[2] Martina Müller,[2] Claus M. Schneider,[2] and Chan-Gyu Lee[3]
[1]*Anhui Key Laboratory of Metal Materials and Processing, School of Material Science and Engineering, Anhui University of Technology, Ma-An-Shan, 243002, Anhui, China*
[2]*Institute of Solid State Research IFF-9, Research Centre Jülich, D-52425 Jülich, Germany*
[3]*School of Nano and Advanced Materials Engineering, Changwon National University, 9 Sarim-dong, Changwon, Gyeongnam, 641-773, Korea*

(Received 6 April 2007; revised manuscript received 23 September 2007; published 19 February 2008)

The valence electronic states at the model tunneling junction interface MgO/Fe(001) system were systematically studied by comparing the spin-resolved photoemission spectroscopy of clean Fe(001) and MgO covered MgO/Fe(001) surfaces using linearly *p*-polarized light. For the clean Fe(001) film on GaAs(001), five distinct features including bulk and surface-related transitions are found. The bulk and surface-state transitions are well-accounted for by the direct transition model based on the calculated energy band structure of bcc bulk Fe(001). The previously observed minority feature at a binding energy $E_B=-1.3$ eV is reinterpreted as a surface roughness associated transition. Upon the MgO adsorption on Fe(001), the surface-state transitions at $E_B=-0.3$ eV below Fermi energy E_F appearing in both the majority and minority spin spectra at low photon energy (18 eV to 35 eV) were quenched. This is also the first direct experimental evidence of a minority spin surface state located just below the Fermi energy as predicted previously. The bulk states at the MgO/Fe(001) interface exhibit a layer-dependent modification, i.e., the bulk states in the deeper Fe layer(s) remain unaffected, while the states of $\Delta_5^{\downarrow}$ band symmetry in the Fe layer(s) closest to the MgO/Fe(001) interface are strongly modified, in contrast to the states of $\Delta_1^{\uparrow}$ symmetry. As a consequence of this interface effect, the "partial spin polarization" at the Fermi level changes sign from negative to positive values as seen in the spin asymmetry spectra at photon energies of 40 eV and 60 eV. The origin of this spin- and symmetry-dependent modification observed at MgO/Fe(001) interfaces is discussed.

DOI: 10.1103/PhysRevB.77.064421 PACS number(s): 73.20.At, 75.70.Cn, 79.60.−i, 75.70.Rf

I. INTRODUCTION

Recently, magnetic tunnel junctions (MTJs) have generated considerable scientific and technological interest, because of their potential applications in next-generation electronic devices such as read heads for ultra-high density hard disk drives and magnetoresistive random access memories.[1–3] An MTJ consists of two ferromagnetic (*F*) layers separated by an insulating (*I*) barrier layer with a thickness in the nanometer range. Due to this low thickness, electrons can pass through the barrier by quantum mechanical tunneling processes. The prominent feature of an MTJ is the tunneling magnetoresistance (TMR), which is defined as $\mathrm{TMR}=(R_{AP}-R_P)/R_P$ where R_{AP} and R_P correspond to the resistance for antiparallel and parallel alignment of the *F* electrode magnetizations, respectively. High TMR values at room temperature (RT) are desirable for field sensing and magnetic memory applications, because they lead to a greater signal level, thus resulting in lower power consumption, higher speed, and larger design margins for devices. The TMR value is also an important parameter in correlating experimental results with theoretical predictions.[4]

The TMR is related to the spin polarization of the tunneling current and can be described in the simplest approximation by Julliere's model:[5]

$$\mathrm{TMR}=\frac{R_{AP}-P_P}{R_P}=\frac{2P_1P_2}{1-P_1P_2}, \tag{1}$$

where P_1 and P_2 are usually taken as the spin polarization of the density of states (DOS) at the Fermi level in each electrode (1) and (2). The higher the polarization values, the larger should be the TMR. This explains why a lot of previous studies of MTJ systems have been devoted to the search for electrode materials with a high spin polarization [e.g., CrO_2,[6] (half-) Heusler alloys,[7] Fe_3O_4 (Ref. 8)]. In addition to the ferromagnetic electrode materials, the properties of the insulating layer in the MTJ also play an important role in determining the TMR performance of a tunneling structure. In most previously studied MTJ systems the insulating barrier layer was made of amorphous aluminum oxide, because of the relative ease of growing pinhole-free AlO_x films. The highest reported TMR value at RT is about 70% for MTJs with FeCo or FeCoB electrodes.[4,9] These TMR values are generally in agreement with the maximum value predicted from Julliere's model by using the effective spin polarization data obtained for these ferromagnetic electrodes. Recently, epitaxial single crystal MTJs involving MgO tunneling barriers have attracted great interest, and a room temperature TMR value up to 220% has been achieved in Fe/MgO/Fe(001) single crystal MTJs.[10,11] In fact, an extremely high TMR ratio (~1000%) was predicted by theory for this model system.[12,13] The origin of the high TMR ratio in single crystal MTJs is found in the peculiar transport mechanism. Instead of a diffusive tunneling process assumed in Julliere's model coherent tunneling of the electrons at the Fermi energy traveling perpendicular to the interfaces through MgO is held responsible, as proposed by Butler *et al.*[12,13] According to Butler's theory, the TMR effect is governed by the transmittance of the bulk electronic states in the electrodes through the tunnel barrier. Their calcula-

tions revealed that electronic wave functions with Δ_1 symmetry have the highest transmittance in an MTJ with fourfold symmetric crystalline structures, such as the Fe(001)/MgO(001)/Fe(001) junctions.

In principle, the magnitude of the TMR is determined by the electronic structure of the entire MTJ system, including the spin properties at the interface between the F electrodes and the tunneling barrier. It is often observed that interface bonding effects at the transition metal-barrier interface play an important (and sometimes intrinsic) role in determining the magnetoresistance of tunnel junctions.[14–16] Although some previous works have investigated the electronic structure at MgO/Fe(001) interfaces, the nature of the interfacial electronic structure and its role on the spin-polarized tunneling effect through MgO is not well understood yet. In the literature the discussion about the formation of a FeO interface layer between MgO and Fe is still controversial. It was previously reported that the MgO/Fe(001) interface is actually composed of an FeO layer.[17,18] However, other experiments showed no evidence for such an interfacial FeO layer.[19,20] The latter experimental results seem to be also supported by theoretical calculations by Li and Freeman,[21] which predict a weak interaction between a thin Fe(100) layer and the MgO(100) substrate. Another recent total energy calculation by Yu and Kim also finds that a formation of interfacial FeO is suppressed under Mg-rich conditions.[22]

Spin- and angular-resolved photoemission spectroscopy (SARPS) is a particularly powerful technique to probe the spin-dependent electronic structure for multilayered MTJ systems. The issue of the F electrode spin polarization in $F/I/F$ MTJ has become a focus of the recent research interest in MTJ systems. There are several techniques that can be employed to measure the spin polarization, such as the Meservey and Tedrow (MT) approach,[23] the Andreev reflection method,[24] and spin-resolved photoemission spectroscopy. The spin polarization is weighted differently in each technique, as in

$$P = \frac{N_{\uparrow} w_{\uparrow} - N_{\downarrow} w_{\downarrow}}{N_{\uparrow} w_{\uparrow} + N_{\downarrow} w_{\downarrow}}, \tag{2}$$

where $N_{\uparrow\downarrow}$ are the up and down spin densities of states, and $w_{\uparrow\downarrow}$ are their respective weight factors.[25,26] The MT technique of spin-polarized tunneling measures the tunneling spin polarization P_T directly by using superconducting tunneling spectroscopy (STS) in related tunnel junctions, in which one of the ferromagnetic electrodes of the MTJ is replaced by a thin superconducting (S) layer. Here the weights are $w_{\uparrow\downarrow} = v_{x\uparrow\downarrow} T_{\uparrow\downarrow}$, where $v_{x\uparrow\downarrow}$ are the x components of the Fermi velocities for spin up and down electrons, and $T_{\uparrow\downarrow}$ are the transmission coefficients for tunneling through the particular barrier. In Andreev reflection a superconducting point contact is used to determine the spin polarization at the Fermi energy.[24] In that case the weights are $v_{x\uparrow\downarrow}$ or $v^2_{x\uparrow\downarrow}$ for the ballistic and diffusive cases, respectively. By contrast, spin-resolved photoemission measures the unweighted spin polarization of photoexcited electrons at the ferromagnet/vacuum interface. It gives a wave-vector and symmetry-resolved view of the spin polarization at the Fermi level. At the MgO/Fe(001) interface—as the tunneling through the MgO barrier involves mostly electrons with $k_{//}=0$—the normal emission experiments probe the same states relevant for the spin-dependent tunneling. Compared to the other two transport-based techniques, spin-resolved photoemission spectroscopy can provide specific and wave-vector resolved information on the energy band structure for both the magnetic electrode[27] and the insulating barrier,[28] especially the influence of an oxide overlayer on the electronic structure of the F electrodes.[28–30]

Recently, Bataille *et al.*[31] performed spin-resolved photoemission measurements at the $Fe_3O_4/\gamma\text{-}Al_2O_3$ tunneling junction interface. They found a negative spin polarization, which is in contrast to a positive value extracted from tunneling experiments. Due to the different definition of the spin polarization between two techniques, the positive spin polarization measured by tunneling experiment is related to the tunneling process itself, and can thus not be easily ascribed to a change of the surface electronic structure of the Fe_3O_4 electrode after incorporation into a bilayer. Dedkov *et al.*[32] also employed SR-PES to explore the spin polarization at the Fe(110)/a-Al_2O_3 interface and found a negative value of $P \approx -15\%$ near the Fermi energy. This value reflects an attenuation from $P=-80\%$ of Fe(110) by the oxide overlayer. More recently, they found the existence of an interfacial FeO layer for the Fe(110)/MgO interface, when MgO films were grown by exposing the Fe(110) surface to Mg vapor in a controlled oxygen atmosphere at room temperature.[33] On the Fe/MgO(001) interface, Sicot *et al.*[34,35] performed x-ray magnetic circular dichroism (XMCD) measurements on 2 ML MgO/Fe(100) grown on bulk MgO(100). Their results demonstrated that the magnetization at the Fe/MgO(001) interface is larger than in bulk (3 μ_B/at for Fe), which is in agreement with previous theoretical predictions.[21] Besides, a positive spin polarization of $P \approx +42\%$ fully integrated in k space was measured by spin-resolved x-ray photoemission spectroscopy using circularly polarized light.[34] However, the positive sign found for the polarization of MgO/Fe(001) is surprising. For Fe(001) a negative polarization could be expected due to the smaller density of states (DOS) at the Fermi level for the majority spin direction, because the majority d-band is below the Fermi level. In order to get a more realistic understanding of the microscopic origin of transport phenomena in magnetism, it is crucial to investigate the details of the spin-polarized electronic structure at the Fe/MgO(001) interface.

As a first step towards an experimental analysis of the electronic states in Fe/MgO/Fe MTJs, we address the modifications introduced by an MgO overlayer on Fe. In this paper, we will employ linearly p-polarized light to explore the detailed electronic structure in the valence bands of Fe/MgO(001) interface. First, we will present and discuss spin-resolved photoemission results of 15 monolayer thick pure Fe(001) films grown on GaAs(001). The analysis of bulk and surface-related states along the Γ-H symmetry line forms the basis for the subsequent studies of the influence of the MgO overlayer on these states. Our spin-resolved photoemission spectroscopy data reveal a spin and photon energy-dependent attenuation of the Fe(001)-related photoemission

features upon covering with MgO. Our study also provides direct evidence for a stronger modification of the $\Delta_5^{\downarrow}$ bulk states compared to those of $\Delta_1^{\uparrow}$ character. This symmetry-dependent mechanism results in a sign change of the spin polarization at the Fermi level from negative at the Fe(001) surface into positive at the MgO/Fe(001) interface.

II. EXPERIMENTAL DETAILS

A reasonable choice of the substrate to grow the Fe/MgO(001) system is GaAs(001). This is basically motivated by the fact that the lattice constant of bcc Fe (a_0 =2.866 Å) is almost exactly half that of GaAs(001) (a_0 =5.654 Å), and the importance of the Fe/GaAs(001) interface in spin electronics and spin-injection devices.[36,37] Previous studies on the Fe/GaAs(001) system yielded some very promising results. Good-quality Fe thin films with negligible diffusion of As at the interface could be obtained, if the Fe layers were grown on Ga-terminated GaAs(001) substrates.[38,39] A recent *ab initio* calculation in the ballistic limit predicted that perfectly sharp and ordered Fe/GaAs(001) interfaces act like a nearly ideal spin filter with a spin polarization as high as $P=+99\%$, i.e., the charge carriers comprise almost exclusively majority-spin electrons.[40] The good epitaxial properties of Fe on GaAs(001) should make it also possible to study single crystal magnetic heterojunctions grown directly on GaAs(001), such as Fe/MgO/Fe(001).

The samples studied were grown in a dedicated UHV preparation chamber with a base pressure less than 2×10^{-10} mbar. The GaAs(001) wafer (Te-doped *n*-type, doping concentration 10^{17} cm^{-3}) was cut into 10 mm$\times$10 mm chips and cleaned in boiling isopropyl alcohol for 4 min, before loading the chips into the UHV chamber. At first, the GaAs(001) surface was treated by annealing at roughly 500 °C to outgas the sample holder and to desorb hydrocarbons. The second step comprised Ar ion sputtering at 500 eV, followed by a final annealing at about 560 °C. The sputtering procedure was performed at room temperature. Subsequent Auger electron spectroscopy measurements confirmed that oxygen or carbon contaminations had been removed successfully. Figure 1(a) depicts a low energy electron diffraction (LEED) pattern of such well-prepared and cleaned GaAs(100) surfaces. It displays a $p(4\times6)$ reconstruction pattern that is ascribed to a clean flat Ga-terminated GaAs(100) surface.[39,41] The Ga-terminated surface is favored, because it is known to suppress As segregation into the Fe film and to improve the epitaxial growth of iron.[39] On such prepared GaAs substrates 15 monolayer (ML) thick iron films were grown by electron-beam assisted evaporation from an iron rod of high purity (99.995%). Prior to the film growth the iron rod has been carefully degassed in order to remove intrinsic nitrogen contaminations. Subsequent Auger electron spectroscopy measurements revealed no traces of carbon or oxygen contaminations at the iron film surface. The medium energy electron diffraction (MEED) pattern and LEED images at different electron energies indicate a well-ordered body-centered cubic (bcc) iron film, as shown in Figs. 1(b)–1(d), respectively. *In situ* longitudinal magneto-optical Kerr effect (MOKE) measurements (see Fig. 2) showed a uniaxial anisotropy with the easy axis oriented along the [110] direction, which is consistent with previous findings.[42,43]

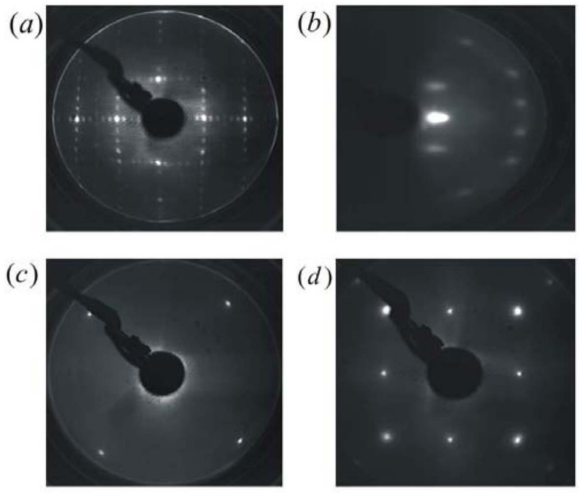

FIG. 1. (Color online) LEED pattern of (a) GaAs(001)-4×6, E=113 eV; (b) MEED pattern of 15 ML Fe/GaAs(001)-4×6 with azimuth along [110], E=3 keV; (c) LEED pattern of 15 ML Fe/GaAs(001)-4×6, E=38 eV; (d) LEED pattern of 15 ML Fe/GaAs(001)-4×6, E=187 eV.

The MgO films were grown by electron-beam assisted evaporation from a magnesium rod and simultaneous oxidation in a controllable oxygen partial pressure, whereby the oxygen was guided through a nozzle directly to the sample surface. In order to avoid overoxidizing the Mg, which would lead to an oxidization of the underlying Fe film, we adjusted the oxygen partial pressure as low as possible during the Mg evaporation. The minimum oxygen partial pressure for the growth of stoichiometric MgO films was found to be 1×10^{-8} mbar. Figure 3 shows some typical Auger spectra for the MgO_x films deposited on Fe/GaAs(001) under various oxygen partial pressures of $p_a=1\times10^{-8}$ mbar, $p_b=3\times10^{-9}$ mbar, and $p_c=1\times10^{-9}$ mbar, respectively. The corresponding evaporating periods for these MgO_x films are t_a=5 min, t_b=4 min, and t_c=6 min, respectively. The Mg evaporation rate is kept constant at 0.1 nm/min. When the

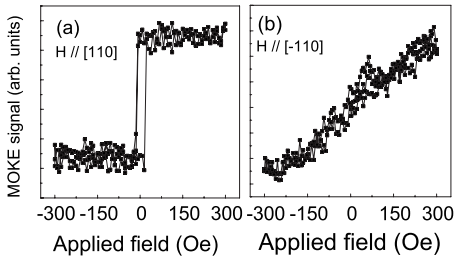

FIG. 2. MOKE loops measured at RT for a 15 ML thick Fe film deposited on GaAs(001): (a) Along the substrate [110] direction (easy-axis of magnetization); (b) along the substrate [−110] direction (hard-axis of magnetization).

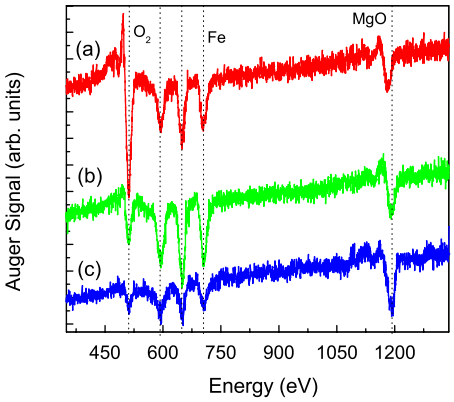

FIG. 3. (Color online) Auger spectrum of MgO_x films deposited on Fe(15 ML)/GaAs(001) using different oxygen partial pressures (a) $p_a=1\times10^{-8}$ mbar, (b) $p_b=3\times10^{-9}$ mbar, and (c) $p_c=1\times10^{-9}$ mbar, respectively. The corresponding evaporation times of the MgO_x films are $t_a=5$ min, $t_b=4$ min, and $t_c=6$ min, respectively. The Mg evaporation rate is kept constant at 0.1 nm/min.

oxygen partial pressure is increased up to $P=1\times10^{-8}$ mbar, a clear chemical shift of the Mg lines due to oxidation was observed (Fig. 3). The composition of the deposited MgO_x film at this oxygen partial pressure ($p=1\times10^{-8}$ mbar) was verified as that of stoichiometric MgO within our experimental uncertainty by comparing the Auger electron spectrum of the oxidized Mg film to a reference taken from of a MgO crystal surface. In contrast to the clear chemical shift for the MgO, we note that the Fe peak positions remain the same independent of the oxygen partial pressures above. This suggests that the underlying Fe film is not oxidized significantly during the MgO growth procedure, although we cannot completely rule out the formation of a minute amount of an interfacial FeO sublayer within our Auger sensitivity (see discussion below). This finding is consistent with the fact that the reactivity of O with Mg is higher than with Fe, because the Fe film is kept at room temperature during the Mg deposition. Thus the as-deposited Mg will immediately react with the adsorbed molecular oxygen on the Fe surface to form MgO. Therefore, we believe that our MgO evaporation procedure has advantages in controlling the interface chemical properties through the choice of the proper oxygen partial pressure, thereby avoiding an overoxidation of MgO and the incorporation of excess oxygen into the Fe interfacial layer.

The thickness d of the MgO film was calibrated by determining the Auger intensities of the Fe LMM Auger transition (I_{Fe}) and Mg core level (I_{Mg}) from the MgO film by combining the following well-known relations:

$$I_{\mathrm{Fe}} = I_0 S_{\mathrm{Fe}} \exp\left(-\frac{d}{\lambda_{\mathrm{Fe}}}\right) \tag{3}$$

and

$$I_{\mathrm{Mg}} = I_0 S_{\mathrm{Mg}} \left[1 - \exp\left(-\frac{d}{\lambda_{\mathrm{Mg}}}\right)\right], \tag{4}$$

where S_{Fe} and S_{Mg} are the sensitivity factors for the corresponding Auger transitions and λ_{Fe} and λ_{Mg} are the attenuation lengths of the Auger electrons originating from Fe and Mg, respectively. I_0 is the primary intensity, which can be eliminated from Eqs. (3) and (4) by considering the Auger signal ratio I_R as

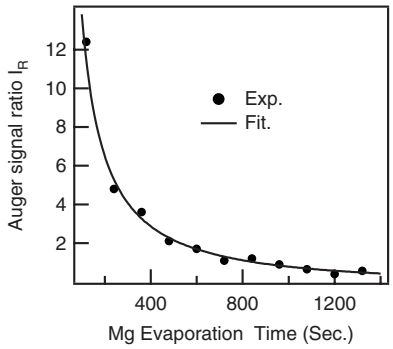

FIG. 4. Auger signal ratio $I_R=I_{\mathrm{Fe}}/I_{\mathrm{Mg}}$ plotted as a function of the Mg evaporation time (full circles) and fit function according to Eq. (5) (further details look text).

$$I_R = \frac{I_{\mathrm{Fe}}}{I_{\mathrm{Mg}}} = \frac{S_{\mathrm{Fe}}}{S_{\mathrm{Mg}}} \frac{\exp\left(-\frac{d}{\lambda_{\mathrm{Fe}}}\right)}{1-\exp\left(-\frac{d}{\lambda_{\mathrm{Mg}}}\right)}. \tag{5}$$

The experimental data set of I_R consists of the peak-to-peak signal ratio of the corresponding Auger transitions of Fe and Mg. Figure 4 shows the Auger signal ratio I_R being plotted versus the deposition time t. TheMgO film thickness is thereby expressed as $d=R\cdot t$, with R denoting the deposition rate. The value of R is determined by a fit of the theoretical curve according to Eq. (5) to the experimental data points (Fig. 4). The fitting parameters of the attenuation lengths of the Auger electrons from Mg and Fe (λ_{Mg} and λ_{Fe}) are taken from experimental values[44] ($\lambda_{\mathrm{Mg}}=1.4$ nm and $\lambda_{\mathrm{Fe}}=1.0$ nm). Thus we extract a value of $R=0.175$ nm/min. It is necessary to mention that the thickness of MgO barrier extracted from the attenuation of Auger electrons is afflicted with an uncertainty that arises from deviations of underlying assumptions, e.g., layer-by-layer growth mode, surface roughness or the chosen values for the attenuation length of the Auger electrons. This uncertainty of the MgO film thickness, however, is not critical for the further discussion of our findings.

The as-grown samples were immediately transferred from the preparation chamber into an adjacent UHV system dedicated to perform photoemission spectroscopy studies. The spin- and angle-resolved photoemission spectroscopy (SR-PES) experiments were accomplished at the undulator beamline U-125-1 PGM (BESSY) offering linear p-polarized light. The angle between incident light and film normal was 45°. In this geometry the electric field vector has components in the sample plane along the [110] direction and parallel to the sample normal [001] as illustrated in Fig. 5(a). Only photoelectrons emitted along the surface normal were analyzed. The photoemission spectra were recorded with the iron films in remanent magnetization. The sample was oriented in such a way that the easy axis [110] was aligned as

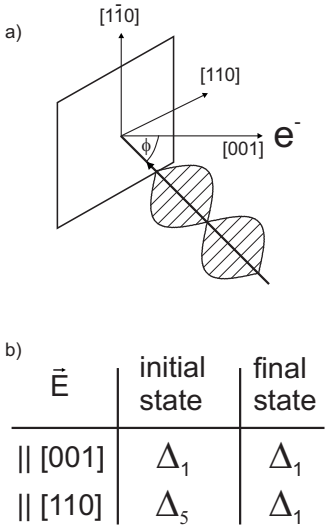

FIG. 5. (a) Illustration of sample geometry: ϕ defines the angle between incident light wave vector and normal direction of the sample. The p-polarized light has electric field components in the plane that is defined by the two orthogonal vectors [110] and [001]. (b) Allowed transitions according the dipole selection rules: A component of the electric field vector E parallel to the [001] ([110]) allows transitions from initial states with Δ_1 (Δ_5) spatial symmetry into final states with Δ_1 spatial symmetry.

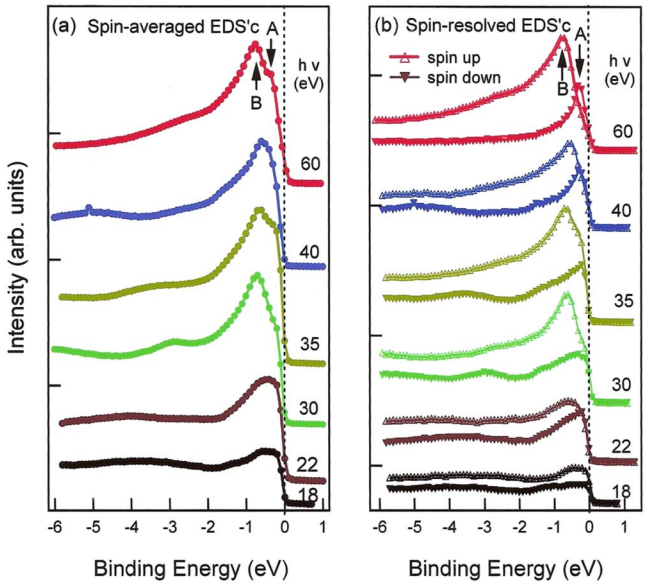

FIG. 6. (Color online) (a) Spin-averaged total intensity I_0 and (b) spin-resolved partial intensities I_+/I_- arrived from photoemission energy distribution curves (EDC's) using photon energies of $h\nu$=18, 22, 30, 35, 40, and 60 eV, respectively.

displayed in Fig. 5(a). The energy of the photoelectrons was determined using a cylindrical mirror type analyzer with integrated LEED spin-polarization detector (CSA200-SPLEED combination.[45])

Each spectrum was measured twice for opposite magnetization directions to eliminate possible apparatus-related asymmetries. An external magnetic field of ~200 mT was applied for the magnetization reversal. The photoemission spectra were recorded with the sample at remanence. The spin polarization P was calculated from the recorded photoemission spectra using a spin sensitivity of S=0.23. From the total intensity I_0 and the spin polarization P, the partial intensities I_+ and I_- with spin-up and spin-down character were derived according to the relations $I_+=I_0/2(1+P)$ and $I_-=I_0/2(1-P)$. The overall energy resolution, which is defined by the spectral resolution of the beamline, the angular acceptance of the entrance electron optics ($\pm 6°$), pass energy of the analyzer, and slit width was set to nominally 200 meV. The spin polarization components of the photoelectrons parallel to the sample normal and in-plane along the [110] direction were determined simultaneously. The k-resolution is determined by the angular acceptance of the analyzer and the kinetic energy of the photoelectrons, e.g., $\Delta k_{||}$=0.2 Å^{-1} for 18 eV photon energy. The displayed spin-resolved photoemission spectra in the paper always depict the spin polarization component of the photoelectron along the [110] direction of the sample (easy axis of the iron film). All measurements were accomplished at room temperature.

III. EXPERIMENTAL RESULTS

A. Fe/GaAs(001)

In Fig. 6 we display the normal photoemission spectra obtained from a 15 monolayer thick (ML) clean Fe(001) film on GaAs(001). The spin-averaged and spin-resolved energy distribution curves (EDC's) for several photon energies between 18 eV to 60 eV are compiled in Figs. 6(a) and 6(b), respectively. As only excited photoelectrons with a wave vector normal to the Fe(001) surface were selected, we probed bulk initial states and possible surface states along the Δ line of the three-dimensional Brillouin zone (BZ), which extends from the zone center Γ to the zone edge H. In order to analyze our data and to determine, how the bulk and surface states evolve along the Γ-Δ-H symmetry line, we are first going to identify transitions originating from bulk states of Fe(001). For this purpose, we performed a spin-polarized relativistic Korringa-Kohn-Rostocker band-structure calculation for bulk bcc Fe(001) (lattice constant 0.286 nm) along the Δ direction using the Munich SPRKKR package.[46] Figure 7 shows the results of this calculation. Although the calculation included spin-orbit coupling, we labeled the bands according to the single group symmetry representations for a bcc crystal along the Δ direction (Δ_1,Δ_2,$\Delta_{2'}$,Δ_5 doubly degenerated) to ease a comparison with TMR calculations.[12] Each band of Δ_i (i=1, 2, 2′, and 5) splits into minority and majority spin subbands, respectively. This labeling is justified, because the spin-orbit coupling in Fe is small, and spin-orbit induced mixing of spin states is confined to hybridization points. At normal emission, the dipole selection rules allow direct transitions from initial states with only Δ_1 (attributed to the out-of-plane component of the electric field vector E) and Δ_5 (attributed to the in-plane component of E) spatial symmetry to final states with Δ_1 spatial symmetry, see Fig. 5(b).[47] In Fig. 7 only the related Δ_1 final state bands accessible in normal emission are displayed. Within the direct transition model, the possible direct transitions at the experimental photon energies of $h\nu$=18 eV, 22 eV, 30 eV, 35 eV, 40 eV, and 60 eV can thus be obtained in the reduced

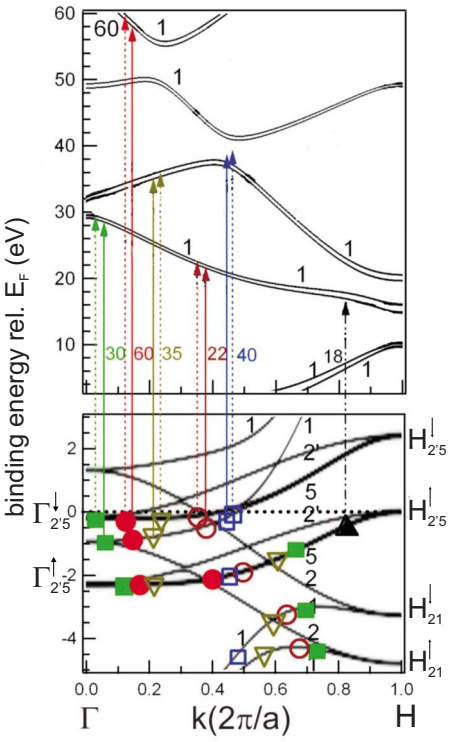

FIG. 7. (Color online) The calculated energy band structure of bulk bcc Fe(001) along the Γ-*H* line. Some representative direct transitions from initial states with $\Delta_5^{\downarrow}$ and $\Delta_1^{\uparrow}$ spatial symmetry into the corresponding final states are suggested by vertical solid and dashed arrows, respectively. The corresponding photon energies are indicated next to the arrows. The marked data points at the $\Delta_5^{\uparrow}$ and the lower lying branch of the Δ_1 symmetry bands suggest initial states excited at photon energies as indicated by the shape of the marked symbols. The horizontal dashed line indicates the Fermi level.

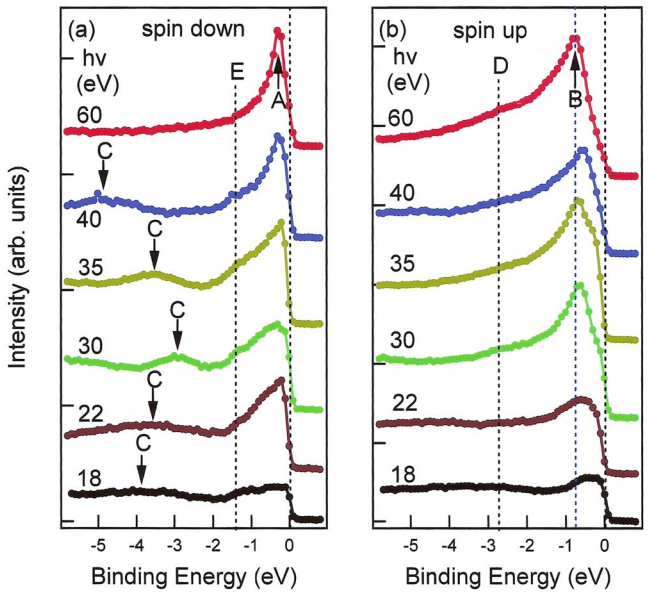

FIG. 8. (Color online) (a) Minority spin and (b) majority spin partial intensities from photoemission spectra measured at photon energy of $h\nu$=18, 22, 30, 35, 40, and 60 eV, respectively.

Brillouin zone representation. Figure 7 displays some representative direct transitions from initial states with $\Delta_5^{\downarrow}$ (or $\Delta_1^{\uparrow}$) spatial symmetry to the corresponding Δ_1 final states. The transitions are indicated by vertical dashed (or solid) arrows with a length corresponding to the photon energy. The assigned photon energy is plotted next to the right-hand side of the line. The dashed (or solid) lines display direct transitions from initial states with spin down (up) character, respectively. In addition, the initial states corresponding to different excitation energy are distinguished by the different symbols used to label the corresponding initial state. Furthermore, initial states for direct transitions from majority states with Δ_5 symmetry and from initial states of the lower lying branch of the Δ_1 symmetry related bands are also plotted in the same way as shown in Fig. 7. The photon energy assigned is denoted by the symbol's shape of the initial state. While we plotted for the initial states the bands of all irreducible representations of the symmetry group C_{4v}, only the final bands of Δ_1 spatial symmetry are displayed in Fig. 7.

The photon energy dependence of the observed photoemission features is more clearly displayed in Fig. 8, where the minority and majority spin EDC's for different photon energies between 18 and 60 eV are compiled separately. In the minority spin channel, there are two main features denoted by peaks "*A*" and "*C*." The intense minority spin feature "*C*" shows a pronounced dispersion with photon energy. The measured peak positions of the minority spin transition "*C*" are consistent with the binding energies of the calculated initial states in the lower lying branch of the $\Delta_1^{\downarrow}$ band for the experimental photon energies as shown in Fig. 7. Thus, based on the direct transition model we attribute this minority feature "*C*" to bulk transitions of bcc Fe(001). As displayed in Fig. 7, the minority spin feature "*A*" at $E_B=-0.3\pm0.2$ eV below Fermi energy also shows a photon energy-dependent variation of the peak intensity. At a photon energy of $h\nu$=60 eV the minority spin peak "*A*" is most intense, while its spectral weight decreases for lower photon energies. One possible reason for this behavior may be the decreasing photoionization cross section for Fe 3*d* orbital for photon energies below 50 eV. In addition, the $\Delta_5^{\downarrow}$ band crosses the Fermi level in the center of the reduced BZ along Δ. The peak position shows no dispersion with photon energy, because of the flat band course below the Fermi level. However, according to the direct transition model the peak "*A*" observed in the spectra at $h\nu$=22 eV, 30 eV, 35 eV, and 40 eV can be ascribed to bulk transitions from initial states with $\Delta_5^{\downarrow}$ symmetry. At a photon energy of 18 eV, the peak intensity at $E_B=-0.3$ eV binding energy decreases significantly. This is consistent with our calculated band structure, which shows that the initial state $\Delta_5^{\downarrow}$ band moves above the Fermi level and that there is no other minority spin direct bulk transition available at this photon energy. Thus, we should not expect any spectral contributions from minority spin bulk bands near the Fermi level. Either there is no initial state available (right side of BZ near *H*) or there is no final state accessible (left side of BZ near Γ). Some tiny peaks observed in the minority spin spectrum for $h\nu$=18 eV at $E_B=-0.3$ eV may be therefore attributed to surface-state related transitions or indirect transitions.

It is necessary to verify the mechanism of a nondispersive minority feature "*E*" located at a binding energy of $E_B = -1.3 \pm 0.2$ eV in the lower photon energy spectra (from $h\nu = 18$ to 40 eV), where surface-related transitions should dominate because of the minimum in the escape depth of the excited photoelectrons. According to our calculated bcc-Fe(001) bulk band structure, there are no minority spin initial states available at this binding energy. So, this small feature cannot be explained by direct transitions within bulk Fe(001). In the literature one finds a controversial interpretation of this peak. Previously, Turner, Donoho, and Erskine[48] also observed this feature by spin-integrated photoemission at lower photon energies from $h\nu = 9$ eV to 18 eV for normal emission (and $h\nu = 16$ eV and 22 eV for off-normal emission) by using an angular resolution of $\pm 1.2°$. They performed several tests to verify the origin of this feature, such as affecting it by gently sputtering (500 eV, 10 $\mu A/cm^2$) and oxygen chemisorption (a few tenths of a monolayer). They found that the intensity of this feature increased and the surface-state emissions at $E_B = -0.3$ eV below Fermi energy were quenched after sputtering or 0.3 monolayer oxygen adsorption. Therefore, they excluded a surface-state origin of this feature and attributed it to the bulk emission from majority spin $\Gamma_{2'5}$ states into an evanescent final state (because the binding energy of this feature ($E_B = -1.3$ eV) obtained from photoemission spectra is in agreement with the position of the majority spin $\Gamma_{2'5}$ state in the calculated bands). However, a spin-resolved normal photoemission measurement on Fe(001) performed by Vescovo *et al.* using an *s*-polarized light at a photon energy of 16 eV suggested that the −1.3 eV feature is of minority spin character. It was reinterpreted as an oxygen-induced, rather than an intrinsic, bulk Fe feature.[49] Up to now the origin of this minority spin spectral feature is still not well understood. Let us go back again to the experimental results obtained for spin-integrated photoemission from Fe(001) by Turner *et al.* In their off-normal emission experiments they probed the *D* line particularly at the $\bar{M}$ point (in the surface Brillouin zone) from the (110) surface with $k_{//} = 1.55$ Å^{-1}. They found that this feature appears with enhanced peak intensity in the *p*-polarization spectra at photon energy of 16 eV and 22 eV for off-normal emission of Fe(001). The binding energy ($E_B = -1.3$ eV) and band symmetry (even-$D_{\downarrow 4}$) obtained from the photoemission data are in good agreement with the calculated bands. These results suggested that the minority spin feature at −1.3 eV is most likely related to off-normal emission contributions from bulk Fe(001) due to surface disorder or roughness. In our experiment, we have observed this minority spin feature in the normal photoemission spectra at photon energies of $h\nu = 18$ to 40 eV, because we use a relatively larger angular acceptance of the entrance electron optics ($\pm 6°$) to increase the photoemission signal. The surface roughness of our sample can be inferred from the LEED image in Fig. 1(d), which shows sharp spots in the ⟨01⟩ directions and a broadening in the ⟨11⟩ direction spots, for which the out-of-plane diffraction condition is not perfectly fulfilled. Without roughness this condition would not have been relevant and sharp ⟨11⟩ spots would be present. The observed pattern indicates that the Fe grows in the expected (001) bcc structure, but with some roughness. The growth mode found by measuring LEED patterns at different energies indicates the presence of terraces or pyramids in the structure, in agreement with results previously found by Gester[50] and Wieldraaijer.[51] The adsorption of MgO on Fe(001) suppresses the surface-state emission at $E_B = -0.3$ eV below Fermi energy effectively, but does not significantly change this minority spin feature at $E_B = -1.3$ eV (see below). Our data provide further evidence that the origin of this feature is a surface roughness associated emission from the top layer(s) of the bulk Fe(001) crystal.

In the majority spin spectra two main peaks were observed within the experimental binding energy and marked as "*B*" and "*D*" [Fig. 8(b)], respectively. Both transitions showed only a weak dispersion with the photon energy. The broad peak "*D*" that is located at a binding energy $E_B = (-2.6 \pm 0.2)$ eV can be ascribed to bulk transitions from the majority spin band with $\Delta_5^{\uparrow}$ symmetry. Figure 7 reveals that there are photon energies at which we can have contributions to peak "*D*" originating from two initial states at different *k* points within the $\Delta_5^{\uparrow}$ band. Besides the influence of the transition matrix elements, these transitions at two different *k* values occurring for one photon energy may be also responsible for the broadening of feature "*D*." At $h\nu = 60$ eV, the peaks of "*A*" at $E_B = -0.3$ eV and "*D*" around $E_B = -2.6$ eV are due to the emission from the exchange-split Δ_5 symmetry bands near the center of Γ point ($\Gamma_{2'5}^{\downarrow}$ and $\Gamma_{2'5}^{\uparrow}$, respectively). The magnitude of the exchange splitting between $\Gamma_{2'5}^{\downarrow}$ and $\Gamma_{2'5}^{\uparrow}$ for 15 ML Fe/GaAs(001) film amounts to (2.3 ± 0.4) eV and is comparable to that of bulk Fe(001) as measured by Kisker *et al.*,[52] indicating that the Fe (15 ML) film has a bulklike magnetic moment, which may be important for applications in spintronics. The photon energy dependence of the peak "*B*" position is also consistent with the dispersion of the initial states as described by the $\Delta_1^{\uparrow}$ symmetry band of bulk Fe(001). At $h\nu = 30$ eV, 35 eV, 60 eV, the peak "*B*" is located at $E_B = (-0.8 \pm 0.2)$ eV, while in the spectra at $h\nu = 18$ eV, 22 eV, and 40 eV the peak position moves slightly to lower binding energies, around $E_B = (-0.5 \pm 0.2)$ eV. At $h\nu = 18$ eV, the majority peak at about $E_B = -0.5$ eV can be attributed to the bulk transition from initial states in the $\Delta_5^{\uparrow}$ band near the *H* point in the Brillouin zone as shown in Fig. 7. Additionally, there is some indication that there is a small majority spin peak at $E_B = -0.3$ eV just below E_F that may originate from surface-related transitions. This will be further discussed in the section below.

Summarizing our findings up to this point, we explored the spin-resolved electronic states in the valence bands of 15 ML Fe(001) film grown on GaAs(001) by means of SR-PES employing linearly *p*-polarized light. We found five main spectral features and compiled their properties in Table I. The binding energy of the bulk initial states of the band symmetry ($\Delta_1^{\uparrow}$, $\Delta_5^{\downarrow}$, and $\Delta_5^{\uparrow}$) and their dispersion obtained from the photoemission data are in good agreement with the calculated bands of bulk Fe(001). The measured exchange splitting of the Δ_5-symmetry bands near the center of the Brillouin zone (at the $\Gamma_{2'5}^{\uparrow}$ and $\Gamma_{2'5}^{\downarrow}$ points) is about $\Delta E = (2.3 \pm 0.4)$ eV, suggesting that the deposited Fe(001) film

TABLE I. Summary of the observed spectroscopic features and their main character. We list the majority or minority spin characters ($\uparrow\downarrow$), the binding energy (E_B), the assignment as surface-state (SS), surface-roughness (SR), or bulk-related (BR) transitions, the bulk initial state (Δ_i) and final state (Δ_f) for BR, the corresponding exciting photon energy ($h\nu$) for the transitions, etc. The Fe/MgO interface effects on the photoemissions of Fe(001), such as moderately modified (MM), strongly modified (SM), or quenched (Q), are also included.

Feature	Spin ($\uparrow\downarrow$)	E_B (eV)	SS/SR/BR	Δ_i	Δ_f	$h\nu$ (eV)	Fe/MgO
A	$\downarrow$	−0.3	BR	$\Delta_5^\downarrow$	$\Delta_1^\downarrow$	22 to 60	SM
B	$\uparrow$	−0.5 to −0.8	BR	$\Delta_1^\uparrow$	$\Delta_1^\uparrow$	22 to 60	MM
C	$\downarrow$	−3.0 to −5.0	BR	$\Delta_1^\downarrow$	$\Delta_1^\downarrow$	22 to 40	MM
D	$\uparrow$	−2.6	*BR*	$\Delta_5^\uparrow$	$\Delta_1^\uparrow$	18 to 60	MM
E	$\downarrow$	−1.3	SR			18 to 40	MM
A	$\uparrow$ and $\downarrow$	−0.3	SS			18 to 35	*Q*

has a bulklike magnetic moment. In addition to the bulk transitions, we also studied the surface-related transitions. The features at a binding energy of E_B=−0.3 eV observed in both the majority and minority spin spectra at photon energy of $h\nu$=18 eV are ascribed to surface-state transitions. This conclusion will be further supported by the analysis of MgO adsorption effect described in the following. The origin of the previously observed minority spin feature at E_B=−1.3 eV is reinterpreted as a surface roughness associated transition from the topmost iron layer.

B. MgO/Fe/GaAs(001)

In view of the insulating nature of pure MgO, no real electronic states exist in this material from the Fermi level down to the upper edge of the valence band of MgO assuming the absence of any impurity states or surface states. Klaua and co-workers reported a band gap value of 5 eV for a two monolayer thick MgO film that increased to 7.6 eV for six monolayers.[53] Thus, it becomes possible to study the modifications of the electronic states involved at the MgO/Fe(001) interface by comparing photoemission spectra from clean and MgO covered Fe surfaces, within the energy window of the MgO band gap. Figure 9 compiles the spin-resolved photoemission spectroscopy data for photon energies between 18 and 60 eV. The spectra of Fe(15 ML)/GaAs(001) and for 1.25 monolayers MgO on Fe(15 ML)/GaAs(001) are indicated in the figure by solid and dashed line, respectively. A similar comparison with a thicker MgO overlayer is shown in Fig. 10. It is interesting to note that the MgO effects observed on the photoemission from clear Fe(001) depend on the spin character as well as the photon energy. The most significant change introduced by the MgO overlayer is a reduction in spectral intensity that can be traced back to the minority spin state "*A*" with $\Delta_5^\downarrow$ symmetry at E_B=−0.3 eV. In comparison, the majority spin peak "*B*" at E_B=−0.8 eV (originating from initial states in $\Delta_1^\uparrow$ symmetry) is merely moderately affected. Some tiny majority and minority spin features at E_B=−0.3 eV appearing in the Fe(001) spectra at lower photon energies are also suppressed. However, the observed spin and photon energy dependent photoemission attenuation effect is surprising, because previous theoretical calculations[21] predicted a charge transfer between iron and oxygen of less than 0.05 eV that render any chemical interaction between Fe and oxygen unlikely. From the following data we can extract more detailed information about this attenuation effect of the photoelectrons in the MgO overlayer.

In order to address the spin and photon energy dependent modification caused by MgO on Fe, the detailed comparison of the spin-resolved photoemission spectra between a clean and MgO covered iron film measured at several typical photon energies are displayed in Figs. 11–13. For 60 eV, the partial intensities of minority and majority spin spectra are shown in Figs. 11(a) and 11(c), while Figs. 11(b) and 11(d) depict the relevant spin polarization. We find that

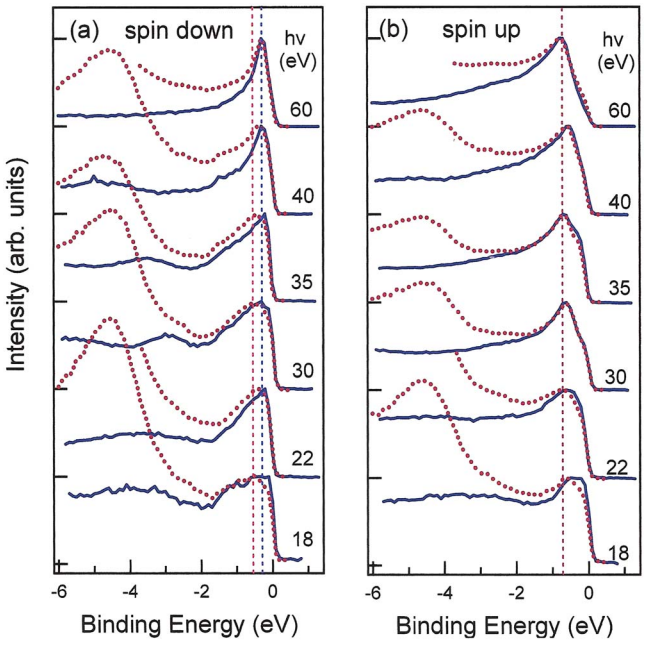

FIG. 9. (Color online) (a) Minority spin and (b) majority spin partial intensities from photoemission spectra of an 1.25 ML nominal thick MgO film on Fe(15 ML)/GaAs(100) (dashed curves) and of an clean Fe(15 ML)/GaAs(001) film (solid curves) for photon energies $h\nu$=18, 22, 30, 35, 40, and 60 eV. The spectra were normalized to the Fe peak as shown in the figure.

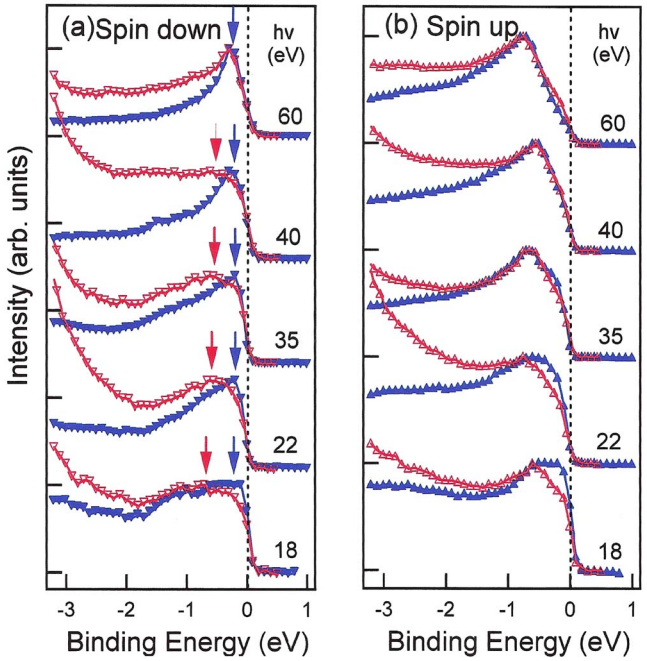

FIG. 10. (Color online) (a) Minority spin and (b) majority spin partial intensities from photoemission spectra of free 15 ML Fe film (solid points), and 2.5 ML MgO/Fe film for photon energies $h\nu$ =60, 40, 35, and 18 eV, and 3.75 ML MgO/Fe sample at $h\nu$ =22 eV (open data points). The spectra were normalized at Fe peak as shown in the figure.

the MgO-related contributions to the photoemission spectra start around 3 eV below the Fermi level reflecting the band gap of the MgO thin film. The majority spin peak "D" at $E_B=(-2.6\pm0.2)$ eV and the minority spin peak "A" at $E_B=(-0.3\pm0.2)$ eV, both of Δ_5 character, are still visible in

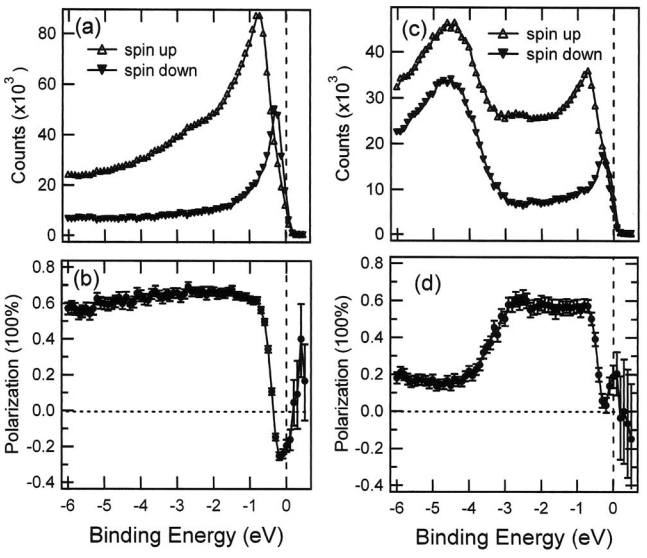

FIG. 11. Spin-resolved partial intensities from photoemission spectra of (a) a clean Fe film (15 ML) on GaAs(001), and (c) a MgO (2.5 ML) covered Fe film (15 ML) on GaAs(001) using a photon energy $h\nu$=60 eV. The lower graphs (b) and (d) display the corresponding spin polarization.

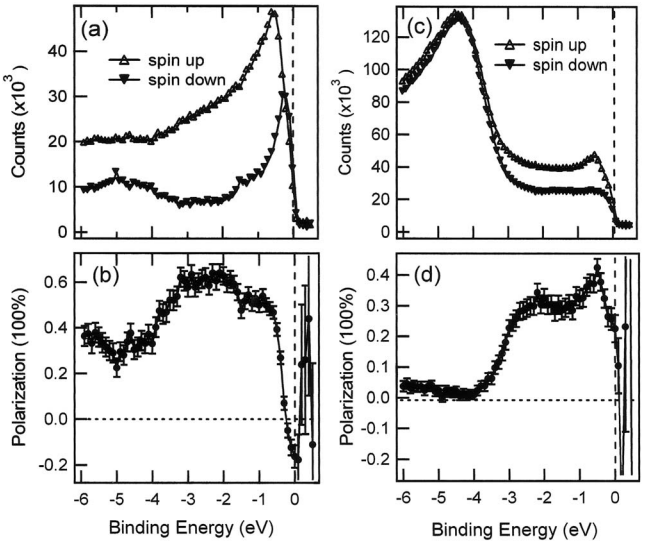

FIG. 12. Spin-resolved partial intensities from photoemission spectra of (a) uncovered Fe film (15 ML) on GaAs(001), and (c) a MgO (2.5 ML) covered Fe film (15 ML) on GaAs(001) using a photon energy $h\nu$=40 eV. The lower graphs (b) and (d) display the corresponding spin polarization.

the spectra of the MgO/Fe(001) sample. We do not find a significant peak position shift within our experimental accuracy. Thus the exchange splitting of the Δ_5 symmetry bands near the center of the Brillouin zone ($\Gamma^{\downarrow}_{2'5}$ and $\Gamma^{\uparrow}_{2'5}$) as deduced from the peak positions remains unchanged. At a photon energy of 60 eV the observed spectra are dominated by the direct transitions from bulk bcc Fe(001) as demonstrated in the above Sec. III. We see that the peak position for the $\Delta^{\uparrow}_1$ and $\Delta^{\downarrow}_5$ symmetry bands did not shift upon the MgO coverage. However, the spin polarization close to the Fermi level at the MgO/Fe(001) interface is clearly modified. For the

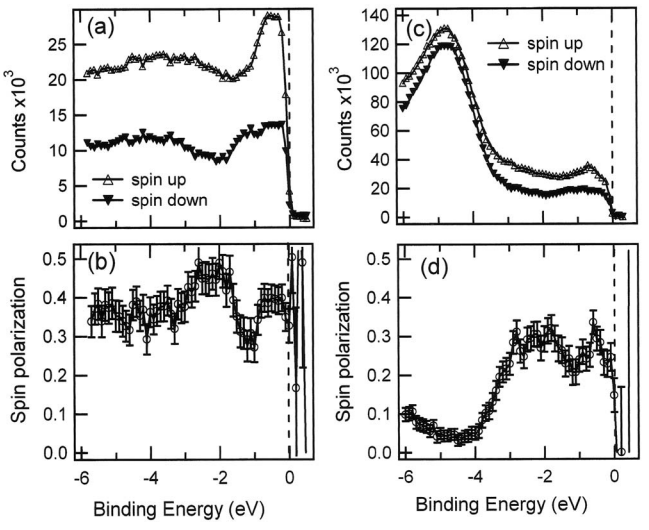

FIG. 13. Spin-resolved partial intensities from photoemission spectra of (a) uncovered Fe film (15 ML) on GaAs(001), and (c) a MgO (2.5 ML) covered Fe film (15 ML) on GaAs(001) using a photon energy $h\nu$=18 eV. The lower graphs (b) and (d) display the corresponding spin polarization.

transitions "*A*" originating from the $\Delta_5^{\downarrow}$ band, located at a binding energy of $E_B=-0.3$ eV, the spin polarization changed significantly from $(-30\pm5)\%$ to $(+20\pm5)\%$. In contrast, the spin polarization value at the binding energy $E_B=-0.8$ eV, that we assigned to transitions from $\Delta_1^{\uparrow}$ in the majority spin spectra, is not affected. Below the binding energy of −3 eV, the spin polarization generally decreases in the case of the MgO/Fe sample, because we have additional contributions from unpolarized photoelectrons originating from MgO. The spin and symmetry-dependent modification of the electronic structure encountered in MgO/Fe(001) can be also be observed in the spectra at lower photon energies discussed in the following.

Figure 12 shows the spin-resolved valence band photoemission spectra measured at a photon energy of $h\nu=40$ eV for clean Fe(001) and MgO(2.5 ML)/Fe(15 ML)/GaAs(001) films. Comparing with the spectra at $h\nu=60$ eV, we can see that the MgO peak is much higher than the Fe peak. This is due to the energy dependence of the photoionization cross section of the oxygen $2p$ and iron $3d$ orbitals. While the photoionization cross section of Fe $3d$ is of the same order for 40 and 60 eV, it strongly drops for O $2p$ from 40 to 60 eV. It is clearly visible that the minority peak at $E_B=-0.3$ eV is almost completely smeared out, while the majority feature at $E_B=-0.8$ eV is only slightly modified upon MgO covering of the Fe(001) surface. As a consequence of this spin and symmetry selective photoemission attenuation, the sign of the spin polarization at the Fermi energy level changes from negative to positive values as shown in Figs. 12(b) and 12(d), respectively.

Compared to the other photon energies, the photoemission spectra at $h\nu=40$ eV reveal the most significant MgO-induced effects. This phenomenon may be related to several factors, such as the photoemission cross section as mentioned above, and the depth-dependent modifications of the electronic structure at the MgO/Fe(001) interface. From our calculated energy band structure of bcc Fe(001), we see that a narrow final-state band gap exists between the band energies of $E_{\text{band}}=37$ and 40 eV above E_F as shown in Fig. 7. At the photon energy of $h\nu=40$ eV, the bulk transitions from the underlying Fe bulk may be partially suppressed due to this band gap. Moreover, the measured spectra may be dominated by surface-related transitions at this excitation energy. Thus it is the most surface-sensitive approach to probe the electronic state modification through atom bonding at the MgO/Fe(001) interface by using photon energies around 40 eV. At higher or lower photon energies, the spectra show a relatively weak modification in the presence of the MgO overlayers, indicating that the measured features at these photon energies are dominated by photoelectrons from the deeper layers in the MgO/Fe/GaAs(001) film system and the electronic structure of these bulk layers is almost not affected by MgO.

Figure 13 shows the spin-resolved photoemission spectra measured at a photon energy of $h\nu=18$ eV for a clean and a MgO covered Fe film, respectively. As already noted in the context of Fig. 6, both majority and minority features located at $E_B=(-0.3\pm0.2)$ eV just below the Fermi level, which have been observed on the clean Fe(001) surface are suppressed. In contrast to the situation at higher photon energies, the attenuation of photoelectrons with majority spin is stronger than that of the minority photoelectrons, resulting in a small decrease of the spin polarization at the Fermi energy. It has been already pointed out in Section A that at a photon energy of 18 eV direct transitions are possible only for majority spin electrons from initial states with $\Delta_5^{\uparrow}$ symmetry character. The corresponding peak is located at a binding energy $E_B=(-0.5\pm0.2)$ eV as indicated in Fig. 7. Thus the suppression of the spectral intensity from both majority and minority spins peaks at $E_B=-0.3$ eV that appeared in the spectra for lower photon energies can be interpreted as a quenching of surface states of bcc Fe(001).

In partial summary, upon covering ultrathin MgO overlayer(s) on bcc Fe(001) surface, a spin- and photon energy-dependent photoemission attenuation is revealed in the SR-PES measurements. The reduction of the transitions at $E_B=-0.3$ eV in both the majority and minority spin spectra at low photon energy ($h\nu=18$ to 35 eV) is ascribed to the quenching of surface states, which is in agreement with above analysis. The surface roughness-associated minority spin transition at $E_B=-1.3$ eV still remains visible without significant modification. The bulk initial states show a layer-dependent modification, i.e., the bulk states in the deeper Fe layer(s) are not affected, contrary to the topmost Fe layer(s) at the MgO/Fe(001) interface. As a consequence of this interface effect, the spin polarization at E_F changes the sign from negative to positive.

IV. DISCUSSION AND CONCLUSION

As we have seen above we cannot assume *a priori* that the electronic states of the clean Fe(100) film will be preserved, if the film is combined with an MgO tunneling barrier and incorporated as an electrode into a Fe/MgO/Fe single-crystalline MTJ. Thus any information concerning the variation of the electronic states induced by oxide overlayers on the Fe(001) surface may be helpful to understand the detailed electronic structure forming at the MgO/Fe(001) interface. Our experiment enabled us to map the main electronic bands with Δ_1 and Δ_5 symmetry along the Δ direction of the Brillouin zone. These symmetries play an important role in the tunneling conductivity of single-crystalline MTJs, as predicted theoretically.[12,13] Our SR-PES study about the electronic structure modification's in MgO/Fe(001) may also be helpful to test the theoretical models for Fe/MgO/Fe MTJs. In general, our SR-PES measurements reveal the main modifications of both bulk and surface states of Fe(001) upon MgO overlayer(s) along the Δ direction.

The spin-polarized electronic surface states are of particular interest as an origin for possible modifications of the magnetic properties with respect to bulk, for example, an enhanced magnetic moment at the surface.[54,55] The early experimental research of the surface electronic structure for Fe(001) was performed by Turner and Erskine by using spin-integrated photoemission spectroscopy. They measured a feature at $E_B=-0.3$ eV in the spectra at low photon energy from 16 eV to 22 eV using polarized light.[56] According to the chosen symmetry and the theoretical predications by

Wang and Freeman,[57] they interpreted this feature as a transition due to a minority spin surface-state which was located just below the Fermi level. On the other hand, the spin- and angle-resolved photoemission spectroscopy measurements performed by Vescovo, Rader, and Carbone, showed that the surface states just below E_F were of majority spin character, rather than a minority surface state. However, the *s*-polarized incident light they used would have been not sensitive to the symmetry connected with the minority SS.[49] Up to now there is still no spin-resolved photoemission data showing evidence for a minority surface states existing just below E_F for the Fe(001) surface.

Our reported spin-resolved photoemission spectra displayed a reduction in the spectral intensity for a low photon energy of 18 eV at $E_B=-0.3$ eV in both spin channels, when we covered the iron surface with MgO. Due to a gap in the Δ_1 final state bands, no direct dipole transitions from bulk Fe states close to E_F in the photon energy range between 10 and 20 eV are possible.[56] Thus, the observation of a decreased spectral intensity can be interpreted as in indication for surface state quenching. Our observation of a majority surface state at $E_B=-0.3$ eV is consistent with the previous experimental work by Vescovo, Rader, and Carbone,[49] and Sawada, Kimura, and Kakizaki.[58] Its existence was also predicted by one-step photoemission calculations performed by Feder *et al.*[59] The minority surface state at $E_B=-0.3$ eV below E_F was predicted in theoretical calculations by Wang and Freeman[57] and should have an even symmetry. Our observation could be a first direct indication for the minority surface state just below Fermi level. In this context, we want to mention reports in the literature stating the presence of a minority surface state just above the Fermi level. Johnson *et al.*[60] performed a spin-polarized photoemission studies of the potassium adsorption on the Fe(001) surface and provided indirect evidence for the presence of a minority-spin surface state located immediately above the Fermi level on the clean surface. Stroscio *et al.* also reported a minority surface state just above Fermi level by using scanning tunneling microscopy (STM).[61] Comparing these different results for the binding energy of the minority SS, one has to keep in mind the different sensitivities of the techniques employed and the experimental conditions under which the Fe films have been prepared and their possible influence on the position of the SS. Thus the conflicting results do not necessarily reflect an inconsistency, but can be rather the result of different positions probed in the two-dimensional Brillouin zone in these experiments.

Our spin-resolved photoemission measurements confirm that the 15 monolayer Fe film deposited on GaAs(001) substrate assumes the electronic band structure of bulk bcc Fe(001). After the iron surface is covered with ultrathin MgO films, the most prominent change in our spectra from MgO/Fe(001), however, is a much stronger modification of the intensity of the $\Delta_5^{\downarrow}$-related spectral features as compared to the majority spin features from the $\Delta_1^{\uparrow}$ band. A similar phenomenon was also observed in the MgO/Co/Fe/GaAs(001) system in our previously published SR-PES work.[27] Again we found that the attenuation of the minority spin states with $\Delta_5^{\downarrow}$ spatial symmetry is much stronger than that of the states with Δ_1 symmetry, although the respective bands in Co are shifted to higher binding energies by about 1 eV, when compared to Fe, and more transitions even with the same spin but different spatial symmetry character occurred in the spectra. Our SR-PES data on both the MgO/Fe(001) and MgO/Co/Fe(001) systems suggest that the modification of the interface electronic states of $\Delta_5^{\downarrow}$-type symmetry is stronger than the one in the Δ_1 symmetry states. This seems to be a common nature for photoemission experiments at the bcc Fe(001) and bct Co(001) surfaces when covered by MgO.

As already mentioned in Sec. I, the SR-PES provides a wave vector and symmetry-resolved view of the spin polarization at E_F for both the clean and MgO-covered ferromagnetic film. At the MgO/Fe(001) interface, the stronger modification of the initial states in $\Delta_5^{\downarrow}$ symmetry just below E_F results in the sign change of the spin polarization at E_F. In contrast to the MgO/Fe(001) system, the spin polarization at E_F for the MgO/Co/Fe(001) system remains at a negative value after covering the bct Co(001) surface with MgO, because the modified $\Delta_5^{\downarrow}$ band is shifted down to higher bonding energies, and the $\Delta_1^{\downarrow}$ band dominates at the Fermi level of bct Co(001) without significant modification. Our photoemission data provide direct evidence that the spin- and symmetry-dependent modification of the electronic band structure at Fermi level plays an important role for the occurrence of the positive spin polarization observed at MgO/Fe(001) interface.

In order to better understand this spin-and symmetry-dependent modification phenomena at the MgO/Fe(001) interface, we should mention several factors which may be held responsible for this behavior. For ultrathin MgO films on Fe(001), modified chemical properties could be expected, because the chemical interaction between MgO and Fe may be enhanced due to the lower coordination of the ultrathin MgO overlayers on Fe. Besides, the interface for the as-deposited MgO/Fe film may still be far from ideal with respect to surface roughness and morphology. This may allow a minute amount of oxygen atoms to occupy the four-fold hollow sites at the Fe surface thereby locally forming in-plane oriented FeO patches, the total amount of which is too small to be detected by Auger spectroscopy or XPS measurements.[34] Thus a formation of "in-plane" FeO would lead to a redistribution of the electron density compared to a clean Fe surface at the Fe-MgO interface. The resulting electron density should be confined entirely within the FeO layer, leaving very few electrons between the Fe atom and the MgO layer.[13] Figure 2 of Ref. 13 displays that a formation of "in-plane" FeO will reduce the majority Δ_1 electron density in the interlayer region between FeO layer and MgO. In this case, one may expect that the impact of the Fe-O bonds on the majority spin states in a Δ_1 symmetry (s,p_z,d_z) band will be much larger than that on the minority spin states of Δ_5 band. Our experimental finding of an only moderate modification of the majority Δ_1 peak indicates that the modification of electronic state due to an "in-plane" FeO formation can be neglected.

Previous studies on the O/Fe(001)-(1×1) interface showed that the first Fe-interlayer expansion is about 23% by

theory[62] and 8% by experiment.[63] Meyerheim *et al.*[17] found an expansion of the first Fe interlayer distance of 16% in the Fe/FeO/MgO system. This upward shift of the Fe surface (as well as subsurface) layers leads to a narrowing and localization of the surface and subsurface *d* states through hybridization. It also leads to a significant loss of the minority spin density and consequently a large enhancement of the magnetic moments in the Fe surface and subsurface layers.[62] The latter was also confirmed recently by x-ray magnetic circular dichroism measurements on MgO/F(001) system.[34] Therefore, an upward shift of the Fe surface (as well as subsurface) layers would modify the overlap of neighboring wave functions. This may lead to a rearrangement of the occupation and thus to a change of the spectral intensities in our measured photoemission data.

Furthermore, the quenched minority surface state due to interface roughness at MgO/Fe(001) may also provide a partial contribution to the spin- and symmetry dependent photoemission attenuation. For the epitaxial Fe/MgO/Fe(001) system, electronic band structure calculations[12,64] have predicted the existence of interfacial resonance states (IRS) that should dominate the minority tunneling conductance.[65,66] Such conduction channels evoked by interfacial resonance states could also mediate the antiferromagnetic (AF) coupling interaction observed in Fe/MgO/Fe(001) junctions.[67,68] In experiments, interfacial resonance states located in the minority band of Fe(001) have been probed by scanning tunneling spectroscopy in high-quality Fe/MgO/Fe epitaxial MTJs, which had an extremely flat bottom Fe/MgO interface.[16] In MTJs, the occurrence of IRSs can be influenced via the topological quality of the Fe/MgO interface. In order to achieve atomically flat Fe/MgO interfaces a postannealing procedure is needed after the growth of the Fe bottom electrode. Otherwise the IRS may be quenched by roughness-related disorder that breaks the local symmetry.[16] Such a postannealing is not possible in our systems, because it would cause a strong diffusion of As into the Fe film. Therefore, our experimental data strongly suggest that the Fe/MgO interface state is indeed quenched after MgO deposition if the Fe surface is not post-annealed. This is another indication that the interface quality is very important for the TMR properties of MTJs. Changing the interface properties in a controlled manner can be utilized to improve the performance of MTJs. A further example of tailoring the properties of MTJs is to introduce an epitaxial monolayer of Ag at the Fe/MgO interface. Belashchenko and co-workers suggested that the presence of the Ag layer should suppress the tunneling conductance channel via the interfacial resonance states[66] and thus may increase the TMR for thinner MgO barriers.

In summary, the valence band electronic states at the MgO/Fe(001) interface were systematically studied by comparing the spin-resolved photoemission spectroscopy of clean and MgO-covered Fe(001) surfaces using linearly *p*-polarized light. For the clean Fe(001) film on GaAs(001), five spectral features reflecting bulk, surface-state and surface roughness associated photoemission contributions are observed. The bulk and surface-state transitions are well accounted for within the direct transition model based on the calculated energy band structure of bulk bcc-Fe(001). According to our findings, the previously observed minority feature at $E_B=-1.3$ eV should be reinterpreted as a surface roughness associated transition. Upon MgO adsorption, the surface-state transitions from Fe(001) at $E_B=-0.3$ eV below E_F appearing in both majority and minority spin spectra at low photon energy (18 eV to 35 eV) were quenched. This is the first direct experimental evidence of a minority surface state sitting just below Fermi energy as predicted previously. The bulk states at the MgO/Fe(001)interface show a layer and band symmetry dependent modification. As a consequence of this interface effect, the spin polarization at the Fermi level changes the sign in the photoemission spectra. This spin and symmetry dependent modification observed at MgO/Fe(001) as well as at MgO/Co/Fe(001) interfaces appears to be a general feature of these type of ferromagnet/insulator systems.

ACKNOWLEDGMENTS

The authors would like to thank the BESSY staff for support during the experiments. The work is financially supported by the Deutsche Forschungsgemeinschaft through Grant No. Schn-353/12, the Scientific Research Foundation for the Returned Overseas Chinese Scholars, State Education Ministry, and the Natural Science Foundation of Education Commission of Anhui Province, China (Grant No. 2005KJ037ZD). One of the authors's work (C.-G.L.), is supported by the International Cooperation Research Program of the Ministry of Science & Technology, Korea.

*Corresponding author. lntong@ahut.edu.cn

[1] J. S. Moodera, L. R. Kinder, T. M. Wong, and R. Meservey, Phys. Rev. Lett. **74**, 3273 (1995).
[2] G. A. Prinz, Science **282**, 1660 (1998).
[3] W. J. Gallagher and S. S. P. Parkin, IBM J. Res. Dev. **50**, 5 (2006).
[4] D. Wang, C. Nordman, J. M. Daughton, Z. Qian, and J. Fink, IEEE Trans. Magn. **40**, 2269 (2004).
[5] M. Jullieère, Phys. Lett. **54A**, 225 (1975).
[6] J. S. Parker, P. G. Ivanov, D. M. Lind, P. Xiong, and Y. Xin, Phys. Rev. B **69**, 220413(R) (2004).
[7] Y. Sakuraba, M. Hattori, M. Oogane, Y. Ando, H. Kato, A. Sakuma, T. Miyazaki, and H. Kubota, Appl. Phys. Lett. **88**, 192508 (2006).
[8] D. J. Huang, C. F. Chang, H.-T. Jeng, G. Y. Guo, H.-J. Lin, W. B. Wu, H. C. Ku, A. Fujimori, Y. Takahashi, and C. T. Chen, Phys. Rev. Lett. **93**, 077204 (2004).
[9] J. Joshua Yang, Chengxiang Ji, Y. Austin Chang, Xianglin Ke, and M. S. Rzchowski, Appl. Phys. Lett. **89**, 202502 (2006).
[10] S. S. P. Parkin, C. Kaiser, A. Panchula, P. M. Rice, B. Hughes, M.

Samant, and S.-H. Yang, Nat. Mater. **3**, 862 (2004).
[11] S. Yuasa *et al.*, Nat. Mater. **3**, 868 (2004).
[12] W. H. Butler, X.-G. Zhang, T. C. Schulthess, and J. M. MacLaren, Phys. Rev. B **63**, 054416 (2001).
[13] X.-G. Zhang, W. H. Butler, and Amrit Bandyopadhyay, Phys. Rev. B **68**, 092402 (2003).
[14] J. M. De Teresa *et al.*, Science **286**, 507 (1999).
[15] T. Nagahama, S. Yuasa, E. Tamura, and Y. Suzuki, Phys. Rev. Lett. **95**, 086602 (2005).
[16] C. Tiusan, J. Faure-Vincent, C. Bellouard, M. Hehn, E. Jouguelet, and A. Schuhl, Phys. Rev. Lett. **93**, 106602 (2004).
[17] H. L. Meyerheim, R. Popescu, J. Kirschner, N. Jedrecy, M. Sauvage-Simkin, B. Heinrich, and R. Pinchaux, Phys. Rev. Lett. **87**, 076102 (2001); H. L. Meyerheim, R. Popescu, N. Jedrecy, M. Vedpathak, M. Sauvage-Simkin, R. Pinchaux, B. Heinrich, and J. Kirschner, Phys. Rev. B **65**, 144433 (2002).
[18] C. Tusche, H. L. Meyerheim, N. Jedrecy, G. Renaud, A. Ernst, J. Henk, P. Bruno, and J. Kirschner, Phys. Rev. Lett. **95**, 176101 (2005).
[19] M. Sicot, S. Andrieu, C. Tiusan, F. Montaigne, and F. Bertran, J. Appl. Phys. **99**, 08D301 (2006).
[20] L. Plucinski, Y. Zhao, B. Sinkovic, and E. Vescovo, Phys. Rev. B **75**, 214411 (2007).
[21] C. Li and A. J. Freeman, Phys. Rev. B **43**, 780 (1991).
[22] B. D. Yu and J.-S. Kim, Phys. Rev. B **73**, 125408 (2006).
[23] R. Meservey and P. M. Tedrow, Phys. Rep. **238**, 173 (1994).
[24] R. J. Soulen, Jr., J. M. Byers, M. S. Osofsky, B. Nadgorny, T. Ambrose, S. F. Cheng, P. R. Broussard, C. T. Tanaka, J. Nowak, J. S. Moodera, A. Barry, and J. M. D. Coey, Science **282**, 85 (1998).
[25] I. I. Mazin, Phys. Rev. Lett. **83**, 1427 (1999).
[26] D. C. Worledge and T. H. Geballe, Phys. Rev. Lett. **85**, 5182 (2000).
[27] Liu-Niu Tong, Cai-Lian Deng, Frank Matthes, Martina Müller, Claus M. Schneider, and Chan-Gyu Lee, Phys. Rev. B **73**, 214401 (2006).
[28] Y. Z. Wu, A. K. Schmid, and Z. Q. Qiu, Phys. Rev. Lett. **97**, 217205 (2006).
[29] F. Matthes, L.-N. Tong, and C. M. Schneider, J. Appl. Phys. **95**, 7240 (2004).
[30] Martina Müller, Frank Matthes, and Claus M. Schneider, J. Appl. Phys. **101**, 09G519 (2007).
[31] A. M. Bataille, A. Tagliaferri, S. Gota, C. de Nadaï, J.-B. Moussy, M.-J. Guittet, K. Bouzehouane, F. Petroff, M. Gautier-Soyer, and N. B. Brookes, Phys. Rev. B **73**, 172201 (2006).
[32] Yu. S. Dedkov, M. Fonin, U. Rüdiger, and G. Güntherodt, Appl. Phys. Lett. **81**, 2584 (2002).
[33] Y. S. Dedkov, M. Fonin, U. Rüdiger, and G. Güntherodt, Appl. Phys. A: Mater. Sci. Process. **82**, 489 (2006).
[34] M. Sicot, S. Andrieu, P. Turban, Y. Fagot-Revurat, H. Cercellier, A. Tagliaferri, C. De Nadai, N. B. Brookes, F. Bertran, and F. Fortuna, Phys. Rev. B **68**, 184406 (2003).
[35] M. Sicot, S. Andrieu, P. Turban, Y. Fagot-Revurat, H. Cercellier, A. Tagliaferri, C. Denadai, N. B. Brookes, F. Bertran, and F. Fortuna, IEEE Trans. Magn. **40**, 2305 (2004).
[36] A. Filipe, A. Schuhl, and P. Galtier, Appl. Phys. Lett. **70**, 129 (1997).
[37] J. S. Claydon, Y. B. Xu, M. Tselepi, J. A. C. Bland, and G. van der Laan, Phys. Rev. Lett. **93**, 037206 (2004).
[38] Y. B. Xu, E. T. M. Kernohan, D. J. Freeland, A. Ercole, M. Tselepi, and J. A. C. Bland, Phys. Rev. B **58**, 890 (1998).
[39] M. Zolfl, M. Brockmann, M. Kohler, S. Kreuzer, T. Schweinbock, S. Miethaner, F. Bensch, and G. Bayreuther, J. Magn. Magn. Mater. **175**, 16 (1997).
[40] O. Wunnicke, Ph. Mavropoulos, R. Zeller, P. H. Dederichs, and D. Grundler, Phys. Rev. B **65**, 241306(R) (2002).
[41] T. L. Monchesky, B. Heinrich, R. Urban, K. Myrtle, M. Klaua, and J. Kirschner, Phys. Rev. B **60**, 10242 (1999).
[42] M. Madami, S. Tacchi, G. Carlotti, G. Gubbiotti, and R. L. Stamps, Phys. Rev. B **69**, 144408 (2004).
[43] R. Moosbuhler, F. Bensch, M. Dumm, and G. Bayreuther, J. Appl. Phys. **91**, 8757 (2002).
[44] C. M. Schneider, Ph.D. thesis, Berlin, 1990.
[45] Focus GmbH, Germany.
[46] The Munich SPR-KKR package, version 2.1, H. Ebert *et al.*, http:/olymp.cup.unimuenchen.de/ak/ebert/SPRKKR; H. Ebert, in *Electronic Structure and Physical Properties of Solids*, edited by H. Dreyssé, Lecture Notes in Physics Vol. 535 (Springer, Berlin, 2000), p. 191.
[47] W. Eberhardt and F. J. Himpsel, Phys. Rev. B **21**, 5572 (1980).
[48] A. M. Turner, A. W. Donoho, and J. L. Erskine, Phys. Rev. B **29**, 2986 (1984).
[49] E. Vescovo, O. Rader, and C. Carbone, Phys. Rev. B **47**, 13051 (1993).
[50] M. Gester, C. Daboo, S. J. Gray, and J. A. C. Bland, J. Magn. Magn. Mater. **165**, 242 (1997).
[51] H. Wieldraaijer, J. T. Kohlhepp, P. LeClair, K. Ha, and W. J. M. de Jonge, Phys. Rev. B **67**, 224430 (2003).
[52] E. Kisker, K. Schroder, W. Gudat, and M. Campagna, Phys. Rev. B **31**, 329 (1985).
[53] M. Klaua, D. Ullmann, J. Barthel, W. Wulfhekel, J. Kirschner, R. Urban, T. L. Monchesky, A. Enders, J. F. Cochran, and B. Heinrich, Phys. Rev. B **64**, 134411 (2001).
[54] A. J. Freeman and Ruqian Wu, J. Magn. Magn. Mater. **100**, 497 (1991).
[55] S. Ohnishi, A. J. Freeman, and M. Weinert, Phys. Rev. B **28**, 6741 (1983).
[56] A. M. Turner and J. L. Erskine, Phys. Rev. B **30**, 6675 (1984).
[57] C. S. Wang and A. J. Freeman, Phys. Rev. B **24**, 4364 (1981).
[58] M. Sawada, A. Kimura, and A. Kakizaki, Solid State Commun. **109**, 129 (1999).
[59] R. Feder, A. Rodriguez, U. Baier, and E. Kisker, Solid State Commun. **52**, 57 (1984).
[60] P. D. Johnson, Y. Chang, N. B. Brookest, and M. Weinert, J. Phys.: Condens. Matter **10**, 95 (1998).
[61] J. A. Stroscio, D. T. Pierce, A. Davies, R. J. Celotta, and M. Weinert, Phys. Rev. Lett. **75**, 2960 (1995).
[62] S. R. Chubb and W. E. Pickett, Phys. Rev. Lett. **58**, 1248 (1987).
[63] F. Jona and P. M. Marcus, Solid State Commun. **64**, 667 (1987).
[64] J. Mathon and A. Umerski, Phys. Rev. B **63**, 220403(R) (2001).
[65] O. Wunnicke, N. Papanikolaou, R. Zeller, P. H. Dederichs, V. Drchal, and J. Kudrnovsky, Phys. Rev. B **65**, 064425 (2002).
[66] K. D. Belashchenko, J. Velev, and E. Y. Tsymbal, Phys. Rev. B **72**, 140404(R) (2005).
[67] J. Faure-Vincent, C. Tiusan, C. Bellouard, E. Popova, M. Hehn, F. Montaigne, and A. Schuhl, Phys. Rev. Lett. **89**, 107206 (2002).
[68] C. Tiusan, F. Greullet, M. Hehn, F. Montaigne, S. Andrieu, and A. Schuhl, J. Phys.: Condens. Matter **19**, 165201 (2007).